ELSEVIER

Journal of Alloys and Compounds 253–254 (1997) 221–225

Journal of ALLOYS AND COMPOUNDS

Pressure–composition measurements and microstructural analysis of the Laves phases $Zr(Cr_{0.5}Mo_{0.2}M_{0.3})_2$ with M=Fe, Co, Ni

M. Bououdina, P. de Rango, D. Fruchart, J.L. Soubeyroux

Laboratoire de Cristallographie du CNRS, 25 avenue des Martyrs, 38042 Grenoble Cedex 09, France

Abstract

The Laves phases $Zr(Cr_{0.5}Mo_{0.2}M_{0.3})_2$ with M=Fe, Co, Ni have been synthesised in the hexagonal C14 type structure. Hydrogen absorption–desorption isotherms have been determined by pressure–composition isotherms (P–C–T) within the temperature range 298–423 K. We have observed that for more than 50% of chromium substitution, the compounds always have a relatively high capacity ($H/M>1$). Moreover, some isothermal curves reveal the existence of a sloping plateau. To understand the origin of this plateau, the phase composition and purity of polycrystalline alloys have been checked using SEM and EDX techniques.

Keywords: Isotherms; Laves phase; Zirconium alloys; MH batteries

1. Introduction

The Laves phases compounds ZrM_2 where M is a transition metal (V, Cr, Mn) present interesting hydrogen absorbing properties (high capacity, quick absorption, limited activation process). For applications, compounds must have a high hydrogen capacity, a moderate plateau pressure, a flat plateau and a low hysteresis. The $ZrCr_2H_{3.4}$ compound is not acceptable because of its great hydride stability at room temperature (1.2 kPa) [1,2]. Many studies have been devoted to pseudo-binary alloys in order to improve the plateau pressure characteristics without reducing the hydrogen storage capacity [2–11].

In a previous study of the system $Zr(Cr_{1-x}Mo_x)_2$ for $0\leq x\leq 1$ [11], we have found that the as-cast alloys crystallise in the hexagonal C14-type structure. The pressure–composition isotherms (P–C–T) reveal a high hydrogen capacity ($H/M>1.1$ at room temperature) and a slight increase of the plateau pressure with molybdenum content, but the plateau values remain relatively low. In this work, we have selected the molybdenum composition $x_{Mo}=0.2$, and chromium is replaced by another transition metal in order to increase the plateau pressure.

In this paper, we present the structural parameters of as-cast alloys and their hydrides obtained by X-ray diffraction, the phases composition determined by SEM and EDX techniques and (P–C–T) measurements. The results obtained are discussed with regards to the role of the substituted transition metal on the hydriding and dehydriding properties in relation with potential hydrogen storage applications.

2. Experimental details

The samples $Zr(Cr_{0.5}Mo_{0.2}M_{0.3})_2$ with M=Fe, Co, Ni used in this investigation were synthesised by the induction furnace technique under high argon purity atmosphere and using pure metals (99.9%). The hydrides with maximum hydrogen capacity were prepared using autoclaves (see details in refs. [8–11]). All the samples (alloys and hydrides) were analysed by the X-ray powder diffraction technique using a Philips diffractometer ($\lambda_{Cu}=1.5418$ Å) equipped with a backscattering graphite monochromator and controlled by the MacGonio software. Further characterisation of the local chemical composition was carried out by X-ray fluorescence analysis using a Kevex EDX probe attached to a JEOL A840 scanning electron microscope. The pressure–composition isotherms (P–C–T) were performed within the temperature range 298–423 K using a thermogravimetric apparatus [12]. About 1 g of the pulverised powder was introduced in the high pressure reactor and submitted to a primary vacuum. When the vacuum was about 10^{-3} atm, the device was submitted to a secondary vacuum for 5 h ($p\approx10^{-5}$–10^{-6} atm). One bar of hydrogen gas was admitted into the reactor and then the activation process was initiated. The sample activation consists in performing several absorption–desorption iso-

0925-8388/97/$17.00
PII S0925-8388(96)03027-7

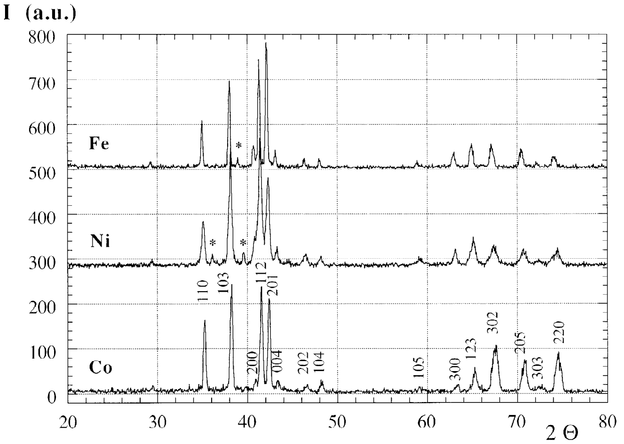

Fig. 1. X-ray powder diffraction patterns of $Zr(Cr_{0.5}Mo_{0.2}M_{0.3})_2$ with M=Fe, Co, Ni as-cast alloys recorded at λ=1.5418 Å (impurities lines are marked with *)

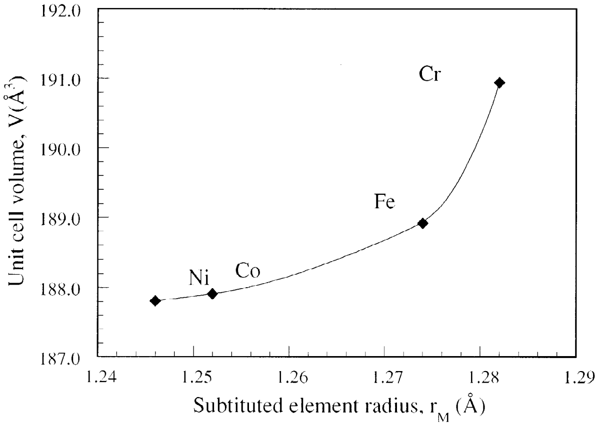

Fig. 2. Variation of the cell volume for the hexagonal C14-type structure versus the atomic radius of the substituted transition metal

bar cycles (the gas pressure and the plateau temperature depend on the sample).

3. Results

3.1. Structural parameters of the alloys and the hydrides

The X-ray diffraction powder patterns (Fig. 1) of the as cast alloys revealed the hexagonal structure with a few extra diffraction lines of low intensity which were analysed by means of SEM and EDX techniques and described latter. The lattice parameters of the alloys and their corresponding hydrides determined from the X-ray powder diffraction data are listed in Table 1.

In Fig. 2 the variation of the alloy unit cell volume with atomic radius of the substituted element is shown. The curve is not linear but it shows an increase of the cell volume with the increase of the substituted atomic radius (r_{Cr}=1.282 Å>r_{Fe}=1.274 Å>r_{Co}=1.252 Å>r_{Ni}=1.246 Å [13]. This behaviour confirms the atomic occupancy of the metal B sites (2a and 6h) by the substituted elements.

The X-ray diffraction patterns of the hydrides show that the initial structure of the parent alloys is conserved after hydrogenation and that the material has been entirely transformed to a β-hydride phase. During the hydride synthesis it has been noticed that the alloys absorb quickly hydrogen and in particular for the sample containing cobalt. The $Zr(Cr_{0.5}Mo_{0.2}Co_{0.3})_2$ sample absorbs immediately hydrogen when gas is admitted into the reactor. The maximum hydrogen content is obtained by measuring the difference in weight of the sample before and after hydrogenation; it depends on the nature of the substituted metal where the larger capacity was found for the nickel substitution (N_H=3.24 H/AB_2) with a volume expansion of 18%.

3.2. Chemical analysis

The alloys show a two-phase equilibrium with dendritic structures with random orientations. Microprobe analysis indicates that both of these two major phases have a Laves $Zr(Cr_{1-x}M_x)_2$ formula, the light grey one being richer in molybdenum than the dark grey one. Other minor phases have been observed for all of them, i.e. an almost pure zirconium phase (white) and some small oxide inclusions (black). For the nickel compound a $Zr_{45}Ni_{55}$ grey phase appears irregularly in small regions. Fig. 3(a to c) show this intergrowth of Laves phases with different molybdenum contents. Table 2 summarises the compositions determined by EDX for the three samples.

Table 1
Cell parameters and hydrogen maximum capacity of alloys and hydrides synthesised in the hexagonal C14-type structure for $Zr(Cr_{0.5}Mo_{0.2}M_{0.3})_2$ with M=Fe, Co, Ni

Alloys	Hydrides							
a (Å)	c (Å)	V (Å^3)	N_H	a (Å)	c (Å)	V (Å^3)	ΔV/V	(%)
$ZrCr_2$ (C14)	5.102(1)	8.294(2)	186.97	3.44	5.385	8.830	221.74	18.60
$Zr(Cr_{0.5}Mo_{0.2}Fe_{0.3})_2$	5.107(1)	8.365(2)	188.92	3.00	5.417(1)	8.866(1)	225.31	19.26
$Zr(Cr_{0.5}Mo_{0.2}Co_{0.3})_2$	5.095(2)	8.360(3)	187.91	2.62	5.354(1)	8.785(2)	218.07	16.05
$Zr(Cr_{0.5}Mo_{0.2}Ni_{0.3})_2$	5.098(1)	8.346(2)	187.809	3.24	5.378(1)	8.824(3)	221.05	17.70

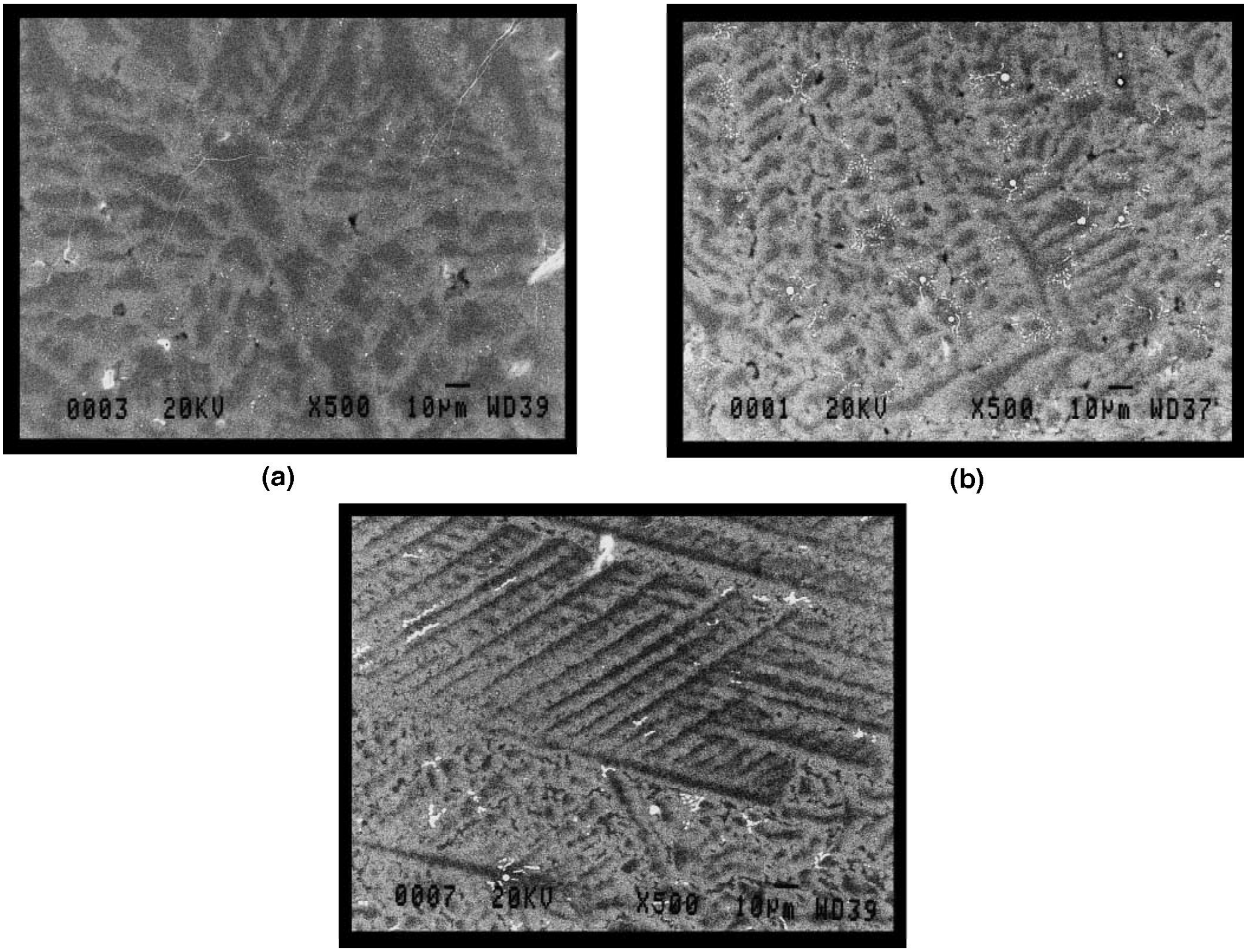

(a) (b) (c)

Fig. 3. (a) Back-scattered electron image of $Zr(Cr_{0.5}Mo_{0.2}Fe_{0.3})_2$ as-cast alloy for a ×500 magnification. (b) Back-scattered electron image of $Zr(Cr_{0.5}Mo_{0.2}Co_{0.3})_2$ as-cast alloy for a ×500 magnification. (c) Back-scattered electron image of $Zr(Cr_{0.5}Mo_{0.2}Ni_{0.3})_2$ as-cast alloy for a ×500 magnification

3.3. Pressure–compositions measurements

Fig. 4(a, b and c) show pressure–composition isotherms for the Fe, Co and Ni substitutions respectively. The P–C–T curves so obtained were measured within the temperature range 298 K to 423 K. It is known that alloying elements and their concentration have strong effects on hydriding properties, but no rule has been established to explain this influence. One of the reasons is that in comparing the various systems, the same substitutional metal can give different and even sometimes opposite effects. For example, the $Zr(Cr_{1-x}Fe_x)_2$ system [3,14,15] exhibits a small hysteresis and a flat plateau in contrast to the $Zr(Mn_{1-x}Fe_x)_2$ system [16].

The isotherms show a fairly good hydrogen capacity, H/M≈1.0 to 1.2 at room temperature. This capacity seems

Table 2
Average atomic compositions observed by means of microprobe analysis on the as cast samples $Zr(Cr_{0.5}Mo_{0.2}M_{0.3})_2$ with M=Fe, Co, Ni

Chemical composition	Dark grey phase	Light grey phase	Other phases
$Zr(Cr_{0.5}Mo_{0.4}Fe_{0.3})_2$	$Zr(Cr_{1.03}Mo_{0.36}Fe_{0.66})$	$Zr(Cr_{1.01}Mo_{0.57}Fe_{0.54})$	Zr, Zr oxide
$Zr(Cr_{0.5}Mo_{0.4}Co_{0.3})_2$	$Zr(Cr_{0.88}Mo_{0.38}Co_{0.51})$	$Zr(Cr_{0.95}Mo_{0.56}Co_{0.36})$	Zr, Zr oxide
$Zr(Cr_{0.5}Mo_{0.4}Ni_{0.3})_2$	$Zr(Cr_{1.06}Mo_{0.50}Ni_{0.48})$	$Zr(Cr_{1.05}Mo_{0.71}Ni_{0.31})$	$Zr_{0.88}Ni_{0.98}$, Zr, Zr oxide

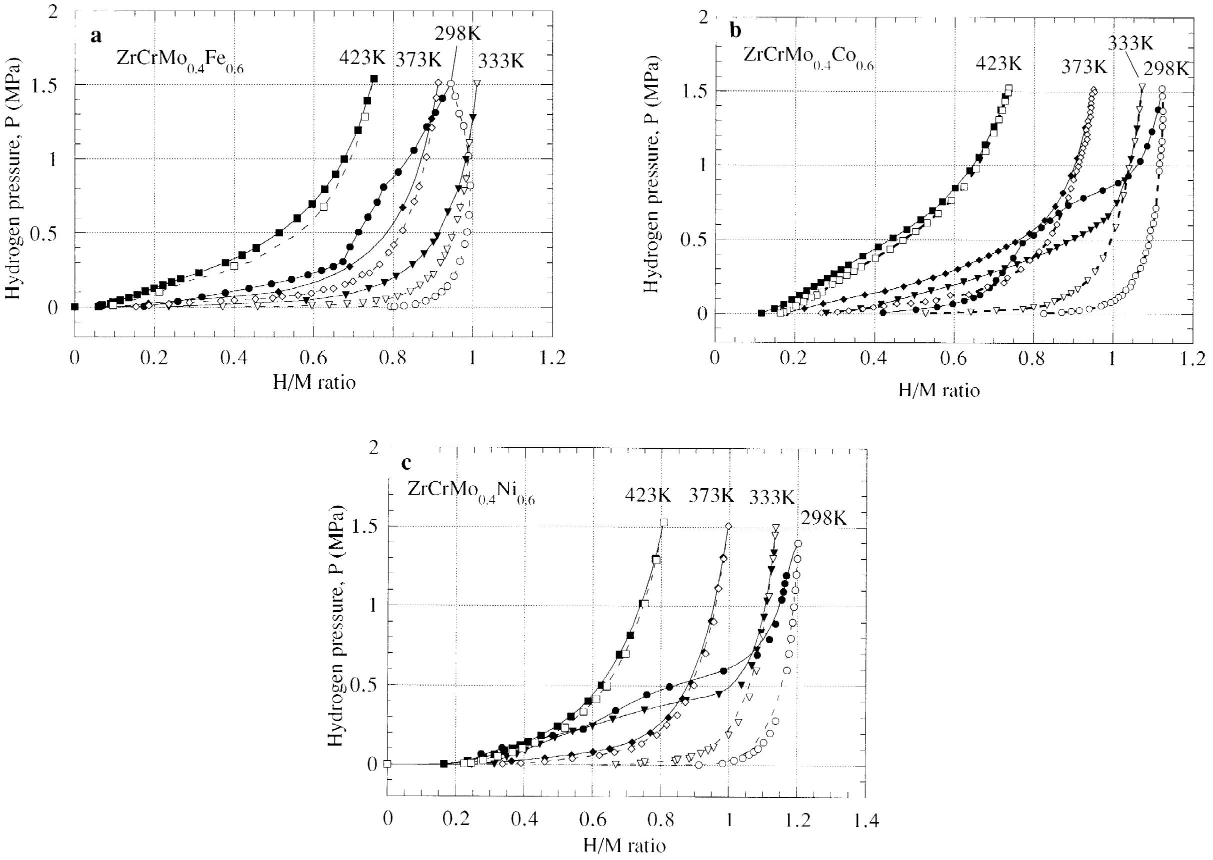

Fig. 4. Pressure–composition isotherms recorded within the temperature range 298–423 K for the respective compositions: (a) $Zr(Cr_{0.5}Mo_{0.2}Fe_{0.3})_2–H_2$; (b) $Zr(Cr_{0.5}Mo_{0.2}Co_{0.3})_2–H_2$; (c) $Zr(Cr_{0.5}Mo_{0.2}Ni_{0.3})_2–H_2$

to be related to the molybdenum as a substituted metal. An increase of the capacity with the atomic number Z of the M substituted element is also observed (at 298 K, $[H/M]^{Fe}=1.0$, $[H/M]^{Co}=1.12$, $[H/M]^{Ni}=1.2$). This capacity decreases with temperature and depends on the nature of the transition metal ($[H/M]^{Fe}_{298}-[H/M]^{Fe}_{423}=0.25$, $[H/M]^{Co}_{298}-[H/M]^{Co}_{423}=0.38$, $[H/M]^{Ni}_{298}-[H/M]^{Ni}_{423}=0.40$).

The analysis of the P–C–T curves indicates the existence of two distinct plateaux. The second plateau may reflect the second Laves phase as observed by SEM and EDX analysis. This plateau pressure value is higher and depends on the transition metal ($P_{plateau}\approx 0.6–0.8$ MPa). The plateau pressure decreases with temperature and this is more pronounced in the case of the nickel compound.

Concerning the plateaux' slope, no important temperature influence or chemical substituted element effect can be observed, except that cobalt seems to give a greater slope than iron or nickel.

For all the compositions, absorption–desorption isotherms show a gradual decrease of the hysteresis width with temperature and the decrease seems to depend on the substituted element M. For example, at 333 K, the hysteresis width decreases in the order: Ni, Fe and Co.

At room temperature, a high stability of the hydrides can be observed from P–C–T curves: the desorption isotherms cease at high H/M ratios (the hydrides can not be fully desorbed). At higher temperature (373 K) hydrogen can be completely released from the β phase hydride and the absorption and desorption isotherms nearly coincide.

4. Conclusion

The $Zr(Cr_{0.5}Mo_{0.2}M_{0.3})_2$ systems with M=Fe, Co, Ni crystallise with the hexagonal C14 Laves phase structure with the presence of a few additional phases. The phase composition analysis carried out on as-cast samples shows the existence of several Laves phases with slightly different compositions.

The pressure–composition isotherms show a high hydrogen capacity, the H/M ratio being between 1.0 and 1.2 at room temperature. The presence of a sloping plateau at high H contents is due to the different Laves composition phases. The value of the plateau pressure depends on the nature of the transition metal M, but this plateau disappears during the desorption cycle.

References

[1] A. Pebler and E.A. Gulbransen, *Electrochem. Technol.*, *4(5–6)* (1966) 211.

[2] D. Shaltiel, I. Jacob and D. Davidov, *J. Less-Comm. Metals, 53* (1977) 117.

[3] S. Qian and D.O. Northwood, *J. Less-Comm. Metals*, *147* (1989) 149.

[4] M. Boulghallat, N. Gerard, O. Canet and A. Percheron-Guegan, *Z. Phys. Chem. NF*, *179* (1993) 171.

[5] A. Drasner and Z. Blazina, *J. Less-Comm. Metals*, *163* (1990) 151.

[6] A. Drasner and Z. Blazina, *J. Less-Comm. Metals*, *175* (1991) 103.

[7] A. Drasner and Z. Blazina, *J. Alloys Comp.*, *199* (1993) 101.

[8] J.L. Soubeyroux, M. Bououdina, D. Fruchart and L. Pontonnier, *J. Alloys Comp.*, *219* (1995) 48.

[9] J.L. Soubeyroux, M. Bououdina, D. Fruchart and P. de Rango, *J. Alloys Comp.*, *231* (1995) 760.

[10] M. Bououdina, J.L. Soubeyroux, D. Fruchart, E. Akiba and K. Nomura, *J. Alloys Comp.*, *235* (1996) 93.

[11] M. Bououdina, P. de Rango, J.L. Soubeyroux, D. Fruchart, E. Akiba and K. Nomura, *J. Alloys Comp.*, (to appear).

[12] M. Bououdina, J.L. Soubeyroux, P. Juen, C. Mouget, R. Argoud and D. Fruchart, *J. Alloys Comp.*, *231* (1995) 422.

[13] E.T. Teatum, K.A. Gschneider and J.T.J. Waber in *Compilation of calculated data useful in predicting metallurgical behavior of the elements in binary alloy systems*, Los Alamos Scientific Laboratory of the University of California, 1968.

[14] S. Qian and D.O. Northwood, *Proc. 5th World Hydrogen Energy Conf., Toronto, July 15–20, 1984*, Pergamon, Oxford, p. 1395.

[15] S. Qian and D.O. Northwood, *J. Mat. Sci. Lett.*, *8* (1989) 418.

[16] V. Shitikov, G. Hilscher, H. Stampfl and H. Kirchmayer, *J. Less-Comm. Metals*, *102* (1984) 29.